 Related Commentary, page 1110

Targeted deletion of *BMK1/ERK5* in adult mice perturbs vascular integrity and leads to endothelial failure

Masaaki Hayashi,[1] Sung-Woo Kim,[1] Kyoko Imanaka-Yoshida,[2] Toshimichi Yoshida,[2] E. Dale Abel,[3] Brian Eliceiri,[4] Young Yang,[5] Richard J. Ulevitch,[1] and Jiing-Dwan Lee[1]

[1]Department of Immunology, The Scripps Research Institute, La Jolla, California, USA. [2]Department of Pathology, Mie University, School of Medicine, Tsu, Mie, Japan. [3]Division of Endocrinology, University of Utah School of Medicine, Salt Lake City, Utah, USA. [4]Cancer Biology, La Jolla Institute for Molecular Medicine, San Diego, California, USA. [5]Johnson and Johnson Pharmaceutical Research and Development, San Diego, California, USA.

Big mitogen-activated protein kinase 1 (BMK1), also known as ERK5, is a member of the MAPK family. Genetic ablation of BMK1 in mice leads to embryonic lethality, precluding the exploration of pathophysiological roles of BMK1 in adult mice. We generated a *BMK1* conditional mutation in mice in which disruption of the *BMK1* gene is under the control of the inducible Mx1-Cre transgene. Ablation of BMK1 in adult mice led to lethality within 2–4 weeks after the induction of Cre recombinase. Physiological analysis showed that the blood vessels became abnormally leaky after deletion of the *BMK1* gene. Histological analysis revealed that, after BMK1 ablation, hemorrhages occurred in multiple organs in which endothelial cells lining the blood vessels became round, irregularly aligned, and, eventually, apoptotic. In vitro removal of BMK1 protein also led to the death of endothelial cells partially due to the deregulation of transcriptional factor MEF2C, which is a direct substrate of BMK1. Additionally, endothelial-specific BMK1-KO leads to cardiovascular defects identical to that of global BMK1-KO mutants, whereas, surprisingly, mice lacking BMK1 in cardiomyocytes developed to term without any apparent defects. Taken together, the data provide direct genetic evidence that the BMK1 pathway is critical for endothelial function and for maintaining blood vessel integrity.

Introduction

MAPKs are common mediators in signal transduction pathways from the membrane to the nucleus in eukaryotic cells. In mammals, four major MAPK pathways have been discovered. They are the extracellular signal-regulated kinases-1 and -2 (ERK1/2), JNKs, p38s, and big mitogen-activated protein kinase-1/ERK5 (BMK1/ERK5) MAPKs. The central part of MAPK cascades is structured by three sequentially activated kinases: a MAPK kinase kinase, or MEKK; a MAPK kinase, or MEK; and a MAPK. These kinase modules relay signals from extracellular agonists to designated cellular targets. We and others have defined a signaling module leading to BMK1 activation, which consists of the kinases MEKK-2/MEKK-3, MEK-5, and BMK1. In response to stimuli these kinases are phosphorylated, directly following a sequential activation (1–4).

MAPK pathways have been shown to mediate proliferation, apoptosis, and differentiation in response to different agonists and in various cellular contexts. Most of these pathways exist in various tissues and perform similar or distinct cellular functions. In previous studies, we, along with other research groups, have demonstrated that the BMK1 signaling pathway is activated by mitogens (1, 5–7) and that this activation is required for growth factor–induced cell-cycle progression from G1 to S phase (5). BMK1 directly activates the MCM1-agamous-deficiens-serum box transcription factors myocyte enhancer factor-2A (MEF2A), MEF2C, and MEF2D and the Ets-domain transcription factor Sap1a. The activation of the MEF2 family of transcription factors leads to the induced expression of c-Jun, which is critical in regulating cell proliferation. In addition, BMK1 activity is critical for neuronal cell survival in retrograde signaling (8, 9), and BMK1 activation promotes the expression of the myosin light chain gene, leading to muscle cell differentiation (10).

Through conventional KO mice, the in vivo function of BMK1 pathway has been implicated in both cardiogenesis and vasculogenesis, causing early lethality around embryonic day 10 (E10) (11, 12). Interestingly, null mutations of the *MEKK3* locus (the upstream regulatory kinase of BMK1) or the *MEF2C* locus (the downstream target of BMK1) both display embryonic defects similar to *BMK1*-null mutant embryos (13–16), which further supports the critical role of the BMK1 pathway in early cardiovascular development. All of these mutant mice also showed impaired extraembryonic development, however, raising the possibility that the cardiovascular defects might be the consequence of a placental defect. Indeed, a recent KO study of p38α, another MAPK, has shown that the vascular defect of the p38α-null embryo appears to be the result of inadequate oxygen and nutrient transfer across the placenta, since after the placental defect was compensated, these embryos developed to term and were normal in morphology (17, 18). Thus, the possible placental defect derived from BMK1 deficiency has to be circumvented to reveal the role of BMK1 in the later stages of mouse development.

Mutants with gene-targeted disruption of key components along the BMK1 signaling pathway (MEKK-3, BMK1, and MEF2C) are

Nonstandard abbreviations used: big mitogen-activated protein kinase-1 (BMK1); $BMK1^{flox/flox}$ Mx1-Cre mice treated with pIpC (BMK1-CKO); cardiomyocyte-specific BMK1-KO (BMK1-cmKO); EC-specific BMK1-KO (BMK1-ecKO); embryonic day (E); endothelial cell (EC); endothelial cell growth supplement (ECGS); extracellular signal-regulated kinases-1 and -2 (ERK1/2); *lacZ*/alkaline phosphatase (Z/AP); MAPK kinase (MEK); MAPK kinase kinase (MEKK); mouse lung capillary endothelial cell (MLCEC); myocyte enhancer factor-2 (MEF2); polyinosinic-polycytidylic acid (pIpC).

Conflict of interest: The authors have declared that no conflict of interest exists.

Citation for this article: *J. Clin. Invest.* **113**:1138–1148 (2004). doi:10.1172/JCI200419890.

embryonic lethal, and the lack of conditional KO models of these molecules has precluded the study of disease processes of this MAPK pathway in the adult stage. Here we have developed an inducible KO mouse model of BMK1 and consequently discovered that the ablation of this MAPK impaired vascular integrity in adult mice. In addition, we show that BMK1 is required for endothelial cell survival and provide a novel genetic model for endothelial failure in adult animals.

Methods

Transgenic mouse lines. ACTB-Flpe, ACTB-Cre, Mx1-Cre, Tie2-Cre (The Jackson Laboratory, Bar Harbor, Maine, USA), and Immortomouse (Charles River Laboratories Inc., Wilmington, Massachusetts, USA) mouse lines have been described (19–23). The αMHC-Cre mouse line (24) was provided by E.D. Abel (University of Utah School of Medicine). The *lacZ*/alkaline phosphatase (Z/AP) mouse line (25) was kindly provided by C. Lobe (Sunnybrook and Women's College, Toronto, Ontario, Canada).

Conditional gene targeting of BMK1. The BMK1 targeting vector was constructed such that exon 4–7 was flanked by a 5′ loxP-containing neomycin resistance gene (*Neo*) cassette and a 3′ loxP site (Figure 1A). Detailed information about the construct is available upon request. Targeted ES cell clones were injected into blastocysts isolated from C57BL/6J mice to produce chimeras. All studies were approved by The Scripps Research Institute Animal Care and Use Committee and comply with NIH guidelines.

Deletion of BMK1 gene by induced Cre-mediated recombination. $BMK1^{flox/flox}$, $BMK1^{flox/+}$, $BMK1^{flox/-}$ mice carrying the Mx1-Cre transgene were injected intraperitoneally with 250 μg polyinosinic-polycytidylic acid (pIpC; Sigma-Aldrich, St. Louis, Missouri, USA) three times at 2-day intervals. The day for the first injection was counted as day 1.

Histological analysis, immunohistochemistry, immunofluorescence, and LacZ/AP staining. Tissues were fixed in 4% paraformaldehyde, dehydrated, embedded in paraffin, sectioned, and analyzed by H&E or trichrome staining. For the CD31 immunohistochemistry study, frozen sections were incubated with primary mAb recognizing CD31 (MEC 13.3; BD Pharmingen, San Diego, California, USA), followed by secondary biotinylated Ab (KPL Inc., Gaithersburg, Maryland, USA). Sections were then processed using an avidin/biotin peroxidase complex method according to the manufacturer's instruction and developed in 3,3′-diaminobenzidinetetrahydrochloride followed by a hematoxylin counterstain. For immunofluorescent studies, sections were stained with a smooth muscle actin Ab (Sigma-Aldrich) followed by Alexa Fluor 488–conjugated IgG (Molecular Probes Inc., Eugene, Oregon, USA) and analyzed using laser-scanning confocal microscope (Bio-Rad Laboratories Inc., Hercules, California, USA). β-Galactosidase and AP staining were performed as described (25).

Electron microscopy. Tissues were processed with 2.5% glutaraldehyde, 4% paraformaldehyde, and 0.02% picric acid in 0.1 M Na-cacodylate. The samples were postfixed with 1% osmium tetroxide and 1.5% ferricyanide, were dehydrated in ethanol, and were infiltrated with Epon resin. Sections were contrasted with lead citrate and viewed on Philips CM-100 electron microscope.

TUNEL staining. Tissue sections were incubated with proteinase K (10 μg/ml) for 10 minutes at room temperature. TUNEL staining was performed using an in situ cell death detection kit (Roche Diagnostics, Mannheim, Germany) according to the manufacturer's instructions. Next, samples were immunostained with anti-CD31 Ab followed by incubation with Alexa Fluor 568–conjugated IgG. For apoptotic endothelial cell (EC) measurements, 10–20 high-powered (×200) fields were randomly selected, and apoptotic ECs were calculated based on the staining of both CD31 and TUNEL-positive cells.

Heart explant cultures. All hearts were aseptically collected from the indicated E9.5 embryos for placement onto hydrated type I collagen gels (rat-tail collagen; Sigma-Aldrich) and cultured for indicated times (26).

Establishment of mouse lung capillary ECs and fibroblast lines. Mouse lung capillary EC (MLCEC) and fibroblast lines were prepared from $BMK1^{flox/flox}$, and $BMK1^{flox/+}$ Immortomice was obtained by crossing BMK1-floxed mice with Immortomice (22). Lungs were isolated, digested with collagenase (1 mg/ml, 37°C, 1 hour) and plated on fibronectin-coated culture plates. After one passage, ECs were purified using anti-CD31 Ab with the magnetic cell-sorting system (MACS; Miltenyi Biotec, Auburn, California, USA). The resulting EC lines had a purity of more than 90% as measured by the uptake of acetylated LDL, by FACS analysis using anti-CD31 Ab, and by immunostaining of vWF. ECs were maintained in MCDB131 medium containing 15% FBS, 90 μg/ml heparin (Sigma-Aldrich), 15 μg/ml EC growth supplement (ECGS; Upstate Biotechnology Inc., Waltham, Massachusetts, USA), and 10 U/ml INF-γ (R&D Systems Inc., Minneapolis, Minnesota, USA) at 33°C. Fibroblast lines were established from the CD31-negative fraction and maintained in DMEM containing 10% FBS and INF-γ (10 U/ml) without heparin and ECGS.

Adenovirus infection, immunoblots, and cell proliferation. Cells were infected with either (or in combination with) Ade, Ade-Cre, and Ade-BMK1 for 12 hours in six-well plates (10^4 particles per cell). Two days after infection, cultured ECs or fibroblasts were lysed in RIPA buffer. The supernatant was separated by SDS-PAGE and probed with Ab's against ERK1/2 and phospho–ERK1/2 (Upstate Biotechnology Inc.), or BMK1. For the proliferation assay, 5×10^4 cells were plated in triplicate into six-well plates and infected with selected adenovirus 20 hours after plating. At various time points cells were stained with crystal violet (Sigma-Aldrich), and the optical density at 590 nm was determined (27). Values were normalized by setting the day 0 culture (20 hours after plating) and the optical density as 1.

Semiquantitative RT-PCR. ECs were infected with Cre-expressing adenovirus and harvested 2 days after infection. Total RNA was purified for RT-PCR. First-strand cDNA was synthesized from these RNAs (1 μg) with the SuperScript Preamplification System kit (Invitrogen Corp., Carlsbad, California, USA). Semiquantitative RT-PCR was performed by a series of fourfold dilutions of the first-strand cDNA (0.1 μg) in each PCR amplification. Sequences for the oligonucleotide primers were described previously (13). The PCR cycle numbers for amplifying specific gene products are 30 (Flt1, Kdr, Tie1, and Tie2), or 23 (β-actin). PCR products were separated by electrophoresis in 1.5% agarose gels and visualized by ethidium bromide staining.

Luciferase assay. The *trans*-reporter plasmid, pG5E1bLuc, and the *cis*-reporter plasmids, pJLuc and pJSXLuc, were described previously (1). For *trans*-reporter systems, pG5E1bLuc and internal control pRL-TK plasmids were cotransfected into cells along with a construct encoding the GAL4-binding domain fused to MEF2C (AA 87–441) (1) transcription factors. For *cis*-reporter systems, cells were cotransfected with either pJLuc or pJSXLuc along with pRL-TK plasmid. Cells were grown on 35-mm multiwell plates and transiently transfected with 1 μg of total plasmid DNA using nucleofection reagent

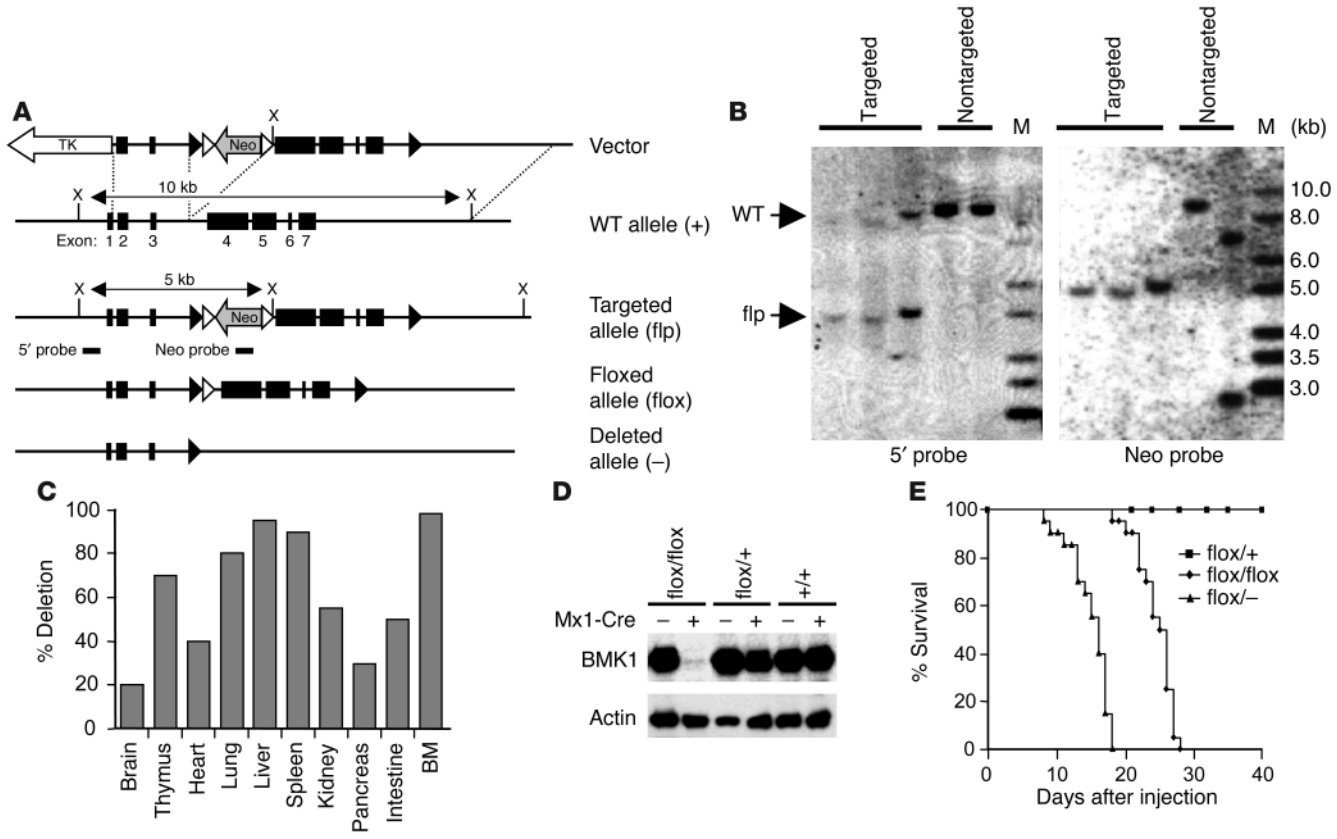

Figure 1
Conditional gene targeting of the *BMK1* gene. (**A**) Diagram of the WT *BMK1* genomic locus (+), the targeted *BMK1* allele (flp), the floxed *BMK1* allele (flox), and the *BMK1* null allele (–). Open and closed arrowheads indicate FRT and loxP sites, respectively. (**B**) Southern blot analysis of targeted ES cell clones. DNAs were digested with XhoI and hybridized with external 5′ probe or internal Neo probe. M, marker. (**C**) Efficiency of Mx1-Cre–mediated *BMK1* deletion in various organs. Hybridization signals from Southern blot analysis were quantified, and the deletion efficiency was calculated as the percentage of signals of deleted alleles in the total signals. BM, bone marrow. (**D**) Immunoblot analysis of BMK1 protein in the livers from pIpC-treated $BMK1^{flox/flox}$, $BMK1^{flox/+}$, and $BMK1^{+/+}$ mice carrying or not carrying the Mx1-Cre transgene as indicated. (**E**) Mortality of BMK1-CKO mice after pIpC treatment: $n = 12$ for $BMK1^{flox/+}$ mice; $n = 20$ for $BMK1^{flox/flox}$ mice; $n = 20$ for $BMK1^{flox/-}$ mice.

(amaxa GmbH, Cologne, Germany). The total amount of DNA for each transfection was kept constant using the empty vector pcDNA3. After 24 hours, the medium was changed to serum-free DMEM. At 48 hours after transfection, the cells were treated with or without stimuli, as described in the figure legends. Luciferase activity was measured using dual-luciferase reporter assay system (Promega Corp., Madison, Wisconsin, USA). The data represent the mean plus or minus SEM of at least three independent transfections.

Apoptosis assay. MLCECs were infected with various recombinant adenoviruses as described above. Seventy-two hours after infection, TUNEL-positive cells were calculated from images captured using a confocal microscope. For transfection experiments using MEF2C-VP16 (a gift from E.N. Olson, University of Texas Southwestern Medical Center, Dallas, Texas, USA), adenovirus-infected MLCECs were harvested 36 hours after infection and electroporated with 10 μg of each mutant and 2 μg green fluorescent protein (GFP) expression vector. Twelve hours after transfection, a 0.6% low-melting-point agarose matrix was overlaid on the cells to prevent loss/dispersion of apoptotic cells. Apoptotic cells expressing GFP were scored based on cellular morphology 24 hours after transfection. To ensure unbiased counting, slides were coded and apoptosis was scored without knowledge of the treatment.

Results

Generation and characterization of mice with a floxed BMK1 allele. We designed a conditional targeting vector for the BMK1 gene in which exons 4–7 of BMK1 gene were flanked by the loxP sequence (Figure 1A). Exon 4 and exons 5–7 code for the kinase domain and unique C-terminal nonkinase region of BMK1, respectively. Both the kinase and C-terminal nonkinase domains are vital for the function and specificity of BMK1. G418/gancyclovir selection for targeting vector–transfected ES cells yielded 738 double-resistant ES cell clones, which were screened for homologous recombination by PCR-based analyses (data not shown) and Southern blot analysis with the 5′ probe and Neo probe (Figure 1B). Three targeted ES cell clones that retained both loxP sites were identified and were used to produce chimeric mice. One of the chimeras transmitted the targeted BMK1 allele through the germ line ($BMK1^{flp/+}$). Next, $BMK1^{flp/+}$ mice were crossed with general deletor mice, ACTB-Flpe, to remove the Neo cassette, which might produce unwanted side effects, by excisional recombination of the Flp/FRT system. The resulting mice, $BMK1^{flox/+}$;ACTB-Flpe, were backcrossed to C57/BL6J mice to segregate the ACTB-Flpe transgene. Mice homozygous for the BMK1-floxed allele were healthy and fertile.

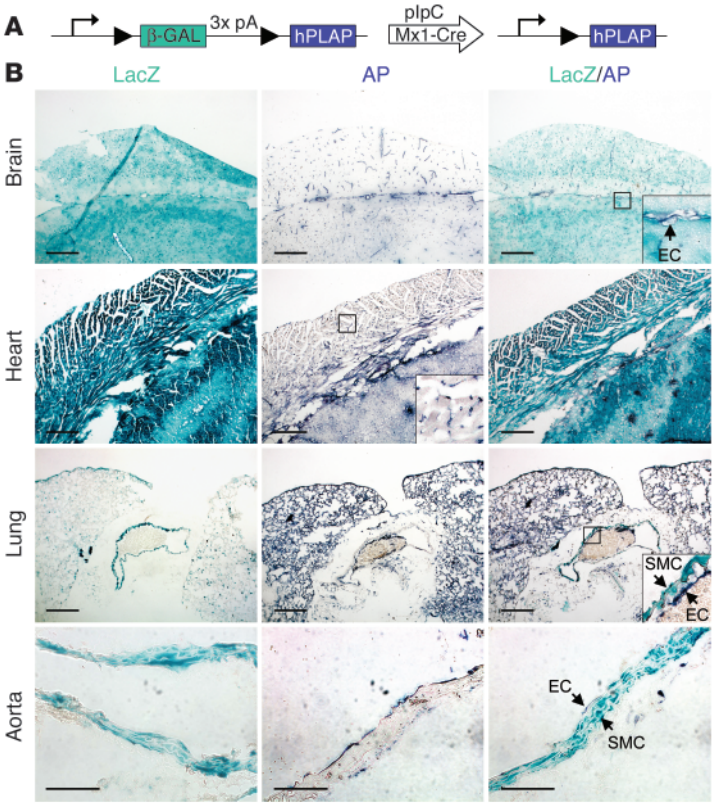

Figure 2
Efficiency of Cre-mediated recombination by induced Mx1-Cre transgene. (**A**) Schematic representation of the expression of Z/AP transgene before and after Cre recombination. (**B**) Sections from pIpC-treated double transgenic (Z/AP, Mx1-Cre) mice were stained for LacZ and/or AP activity. SMC, smooth muscle cell. Scale bars: 50 μm in brain, heart, and lung; 10 μm in aorta.

Inactivating the BMK1 gene in the adult mice. To study the function of BMK1 in adult animals, we chose an inducible gene ablation system, Mx1-Cre, designed to disrupt the *BMK1* gene in adult mice upon pIpC induction (19). Deletion of the *BMK1* gene was achieved by treating 8-week-old $BMK1^{flox/+}$, $BMK1^{flox/-}$, and $BMK1^{flox/flox}$ mice (all carrying the hemizygous Mx1-Cre transgene) with pIpC. The efficiency of recombination in each tissue was examined by Southern blot analysis of tissues harvested from $BMK1^{flox/flox}$ Mx1-Cre mice 1 week after pIpC induction. As shown in Figure 1C, induced recombination was almost complete in the bone marrow, liver, and spleen, whereas the deletion efficiency in other tissues varied from 15 to 80%. The removal of BMK1 protein that resulted from this Cre-mediated recombination was confirmed in the liver of the pIpC-treated $BMK1^{flox/flox}$ mouse carrying the Mx1-Cre transgene (Figure 1D).

Two weeks after induction, the $BMK1^{flox/+}$ mice showed no disease signs, whereas all $BMK1^{flox/flox}$ mice developed a wasting syndrome that was fatal by 3–4 weeks (Figure 1E). The clinical features included dramatic weight loss, dyspnea, and unsteady movements. About 30% of mice ($BMK1^{flox/flox}$) showed hemiparesis with tilted heads. The $BMK1^{flox/-}$ mice died about 10 days earlier than the $BMK1^{flox/flox}$ mice, some without obvious clinical symptoms (Figure 1E). Hereafter, $BMK1^{flox/flox}$ Mx1-Cre mice treated with pIpC are designated as "BMK1-CKO" mice. Histological analysis at 3 weeks after the initial pIpC injection revealed multifocal acute hemorrhages in heart, brain, and lung. Multifocal cellular plaques containing large round cells in the ventricle and diffused degeneration of the myocardial fibers with multifocal inflammatory changes were also observed (data not shown).

Efficient recombination in endothelial cells by Mx1-Cre transgene. Since the level of Mx1-Cre transgene induction varies among tissues after pIpC treatment, we examined whether tissues with highly efficient BMK1 deletion, such as hepatocytes, might acquire their pathogenic properties as the consequence of intrinsic genetic failure. This was achieved by generation of hepatocyte-specific BMK1 KO mice. BMK1 deficiency in this tissue, however, did not influence their survival (data not shown). Therefore, we speculated that there might be other unidentified tissues that have a high efficiency of recombination. To address this issue, Mx1-Cre mice were bred with Z/AP double-reporter mice (25). In these mice, cells express lacZ in the absence of Cre (Figure 2A). In the presence of Cre, however, the *lacZ* gene is excised, and lacZ expression is replaced by AP expression. Interestingly, the expression of AP was observed in all ECs throughout the body, even in tissues with a low efficiency of recombination, such as the brain and heart (Figure 2B). Moreover, no AP expression was observed in cardiomyocytes and smooth muscle cells of blood vessels. These findings indicate that ECs are also an efficient target for this inducible KO system.

Increased vascular leakage after ablation of BMK1. Because Cre-mediated excisional recombination is complete in ECs, we next investigated whether BMK1 ablation has a pathophysiological role in the blood vessels of mutant mice. Evans blue dye was injected into the tail vein of WT and BMK1-CKO mice 1 week after the induction of Cre recombinase, and leakage of dye from the vasculature was examined. The vessels of ear skin in BMK1-CKO mice were abnormally leaky under baseline conditions as judged by Evans blue extravasation (Figure 3, A and B). Moreover, the vascular leakage was further increased in BMK1-CKO mice after topical application of mustard oil, an inflammatory agent that induces vascular leakage and inflammation in the skin (Figure 3, C and D). Spectrophotometric analysis revealed that vascular leakage increased fourfold and threefold in BMK1-CKO mice under baseline and inflamed conditions, respectively (Figure 3E). These findings indicate a role for BMK1 in regulating the integrity of the endothelial barrier in vivo.

Structural integrity of vascular tissues in BMK1-CKO mice. The rapid onset of increased vascular permeability, followed by hemorrhages after BMK1 ablation, prompted us to examine the structural integrity of blood vessels in these mutant mice. Tissue sections from BMK1-CKO hearts and lungs were examined 1, 2, and 3 weeks after the induction of Cre recombinase (Figure 4A). Within the first week of BMK1 ablation in the endocardium, ECs became round and detached from the neighboring cardiomyocytes, suggesting an activation of the cardiac endothelium, a previously described hallmark of endothelial activation (28). In the following week, activated ECs were also observed in blood vessels. Plaques consisted of numerous cells whose relatively large cytoplasms protruded into the lumen. After 3 weeks, severe degeneration of cardiomyocytes was found, possibly due to the massive expansion of these plaques into the cardiac muscles. Similar changes were also observed in the pulmonary endothelium, but less severe than that found in the endocardium or endothelium of the coronary vessels (Figure 4A). Immunohistochemical analysis of heart sections with the EC marker CD31 stained only the surface of these regions but

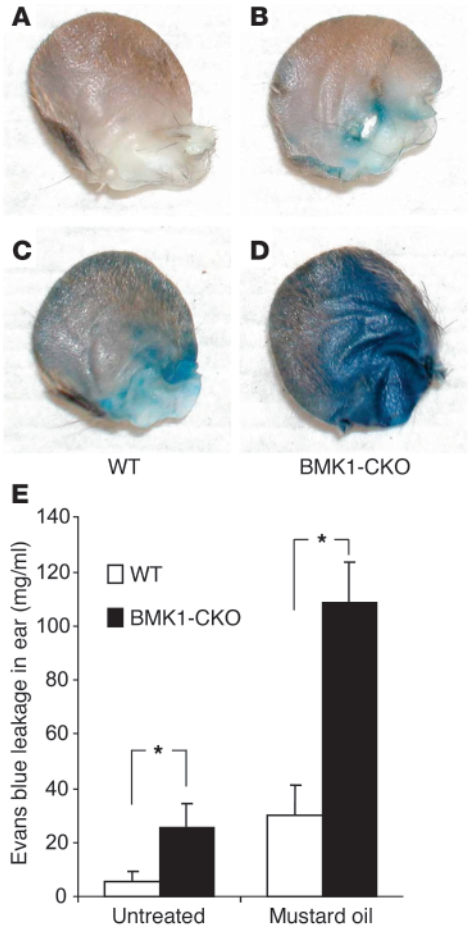

Figure 3
Increased vascular leakage after ablation of BMK1. (**A**–**D**) Representative ears showing increased baseline leakage of Evans blue dye in BMK1-CKO mice, which are further enhanced after topical application of mustard oil. Evans blue dye (30 mg/kg in a volume of 100 μl) was injected into the tail vein of anesthetized mice. (**E**) Quantification of extravasated Evans blue dye. Baseline leakage was elevated in BMK1-CKO mice (black bars) as compared with control WT mice (white bars). Similarly, significant increase in vascular leakage of BMK1-CKO mice was observed after mustard oil treatment. Values are mean ± SEM; $n = 6$ mice per group. $^*P < 0.05$.

did not stain the cellular mass inside (Figure 4B). ECs within major vessels of BMK1-CKO mice were round and irregularly aligned. Moreover, the number of CD31-positive capillaries surrounding the major vessels in the BMK1-CKO heart was much lower than in the control (Figure 4B). In contrast to the potent effect of BMK1 deletion on ECs after pIpC induction, no morphological differences were detected between the VSMCs of mutants versus control animals when tissue sections were stained with an Ab recognizing the smooth muscle actin (Figure 4C).

BMK1 removal leads to apoptosis of ECs in adult animal. To further investigate the blood vessel defect in BMK1-CKO mice, we analyzed their ultrastructure using an electron microscope. Capillaries in control mice were distended with smooth luminal surfaces, whereas capillaries in the BMK1-CKO mice were collapsed with irregular luminal surfaces (Figure 5, A and B). Perinuclear clumping of condensed chromatin, which is an early sign of apoptosis, was detected in some ECs (Figure 5B). Numerous electron-lucent ECs had bulged into the lumen and were also found in the capillaries of BMK1-CKO mice (Figure 5C). These cells contained numerous vesiculovacuolar organelles, which are involved in fluid and macromolecular transport across the endothelium. In contrast to the severe damage observed in the ECs of BMK1-CKO mice, pericytes and cardiomyocytes around these capillaries were relatively well-preserved (Figure 5, B and C). Large fenestrations were also observed in some capillaries just beside the extravasated erythrocytes, suggesting leakage form these portions (Figure 5D).

To determine whether these pathological changes were accompanied by EC apoptosis, TUNEL analysis was combined with CD31 immunofluorescent tissue staining. Few TUNEL-positive cells were found in the hearts of control mice. In contrast, numerous

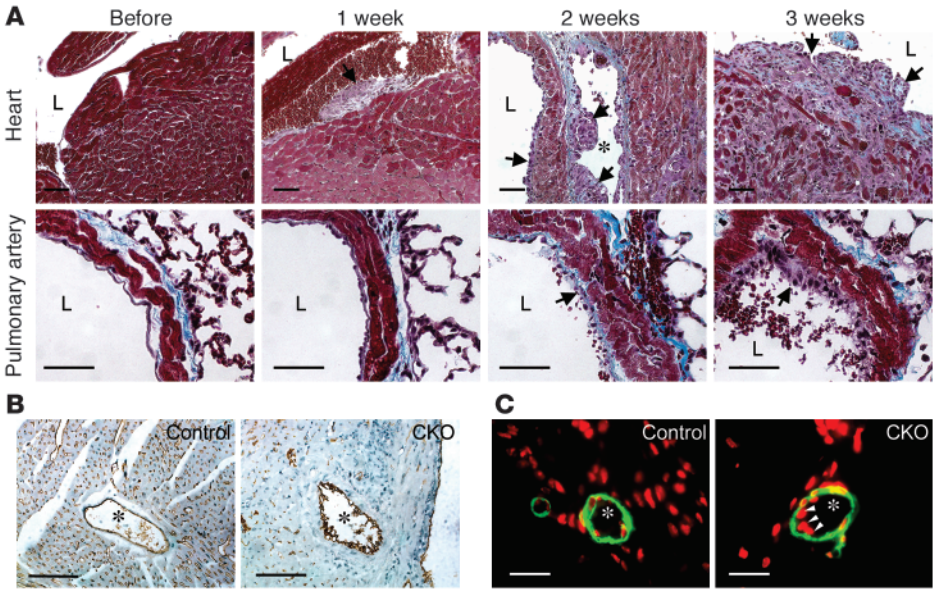

Figure 4
Histopathological analyses of pIpC-treated BMK1-CKO mice. (**A**) Histological analysis of BMK1-CKO hearts and pulmonary arteries at various time points after pIpC treatment. (**B**) Immunohistochemical analysis of control heart (left) and BMK1-CKO heart (right) with the CD31 Ab. (**C**) Immunofluorescent analysis of control heart (left) and BMK1-CKO heart (right) with Ab against smooth muscle actin (green) with nuclear DAPI staining (pseudo-colored, red). Arrowheads indicate abnormal endothelial nuclei. Asterisks indicate coronary arteries. Scale bars: **A** and **B**, 10 μm; **C**, 5 μm.

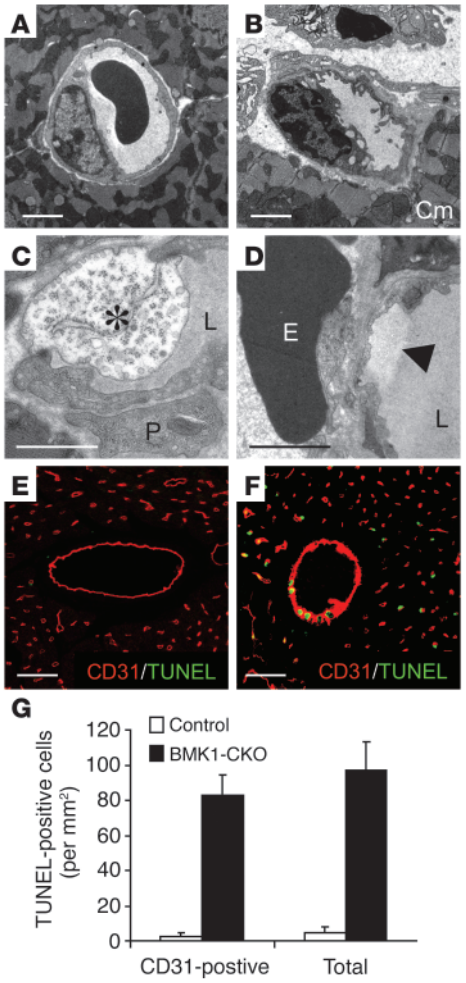

Figure 5
Analysis of apoptotic changes in BMK1-CKO mice. (**A**–**D**) Ultrastructure analyses of capillaries in BMK1-CKO mice. Transmission electron microscopy was performed in the capillaries of control heart (**A**) and BMK1-CKO heart (**B**–**D**). (**E** and **F**) TUNEL and CD31 immunohistochemical staining of heart sections. Confocal immunofluorescent analysis of heart sections stained with CD31 (red) and TUNEL (green) from control mice (**E**) and BMK1-CKO mice (**F**). (**G**) Quantitative analysis of EC apoptosis. Values are mean ± SEM. Asterisk indicates electron-lucent EC. Cm, cardiomyocyte; E, erythrocyte; L, lumen; P, pericyte. Arrow indicates the fenestration of the capillary. Scale bars: **A**–**D**, 2 μm; **E** and **F**, 10 μm.

TUNEL-positive cells colocalized with CD31 immunoreactivity in the hearts of BMK1-CKO mice (Figure 5, E–G). Taken together, these results suggest that *BMK1* ablation leads to EC apoptosis.

EC-specific ablation of BMK1 triggers cardiovascular defects and consequent early death during embryogenesis. To reinforce the notion that BMK1 plays a critical role in endothelial function, we generated EC-specific BMK1-KO (BMK1-ecKO) mutants by crossing BMK1-floxed mice with Tie2-Cre deletor mice. For comparison, we also generated global BMK1-KO ($BMK1^{-/-}$) mutants by breeding $BMK1^{flox/flox}$ mice with ACTB-Cre deletor mice. $BMK1^{-/-}$ mutants died between E9.5 and 10.5, with defects including growth retardation and underdeveloped yolk sac vasculature as compared with WT embryos (Figure 6, A and B). These results are in agreement with the finding of two other groups using conventional targeting strategy to generate BMK1-KO mice (11, 12). Interestingly, BMK1-ecKO mutants also died between E9.5 and 10.5 with identical cardiovascular defects observed in $BMK1^{-/-}$ embryos (Figure 6C). Cross-sections of these yolk sacs revealed that the vasculature in WT yolk sacs were well formed (Figure 6D). The blood vessels in most of the yolk sacs from $BMK1^{-/-}$ and BMK1-ecKO, on the other hand, appeared loose and fragile (Figure 6, E and F). Histological analysis of the hearts from $BMK1^{-/-}$ and BMK1-ecKO mutants at E9.5 revealed that myocardium development was impaired, with reduced trabeculation in the ventricular chamber, when compared with WT embryos (Figure 6, G–I). ECs shaping the endocardium of WT embryos were well extended and produced an even, consistent interior coating for the heart (Figure 6G). On the other hand, the ECs of the mutant endocardium did not produce a smooth inner lining, but were instead irregularly aligned to the myocardium with round-shaped morphology (Figure 6, H and I).

To further examine the endothelial defects in BMK1-ecKO embryos, heart explant cultures from WT and BMK1-ecKO embryos were carried out. In WT heart explants, EC proliferated extensively into the supporting gel matrix and showed mesenchymal transformation at the edge of expansion after culture for 5 days (Figure 6J). Moreover, the myocardium kept contracting rhythmically. In contrast, the ECs of BMK1-ecKO heart explants failed to outgrow into the surrounding gel matrix, suggesting the important role of BMK1 for the proliferation of ECs. Next, we evaluated whether *BMK1*–deficient cardiomyocytes contribute to the cardiac malformation observed in $BMK1^{-/-}$ embryos. To this end, cardiomyocyte-specific BMK1-KO (BMK1-cmKO) mice were generated by crossing BMK1-floxed mice with transgenic mice carrying an αMHC-Cre transgene (24). These mice developed to term and appeared normal for at least 1 year. Histological analysis revealed that there was no difference between the sections isolated from 6-month-old WT and BMK1-cmKO mice (Figure 6, K and L). Taken together, these results suggested that the cardiovascular defects of the $BMK1^{-/-}$ embryo were caused solely by the malfunction of BMK1-deficient ECs.

Essential role of BMK1 in endothelial survival. BMK1 has been shown to be a key mediator for growth factor–induced cellular activation. For the proliferation and survival of ECs, several growth factors, such as VEGF, bFGF, and EGF, are known to be important (28–30). Significant activation of the BMK1 pathway by these growth factors was detected in both MLCECs isolated from $BMK1^{flox/flox}$ mice and human umbilical vein endothelial cells (HUVECs) (Figure 7A and data not shown). Next, the floxed *BMK1* gene was deleted from $BMK1^{flox/flox}$ and $BMK1^{flox/+}$ ECs or fibroblasts by treating cells with recombinant adenovirus encoding Cre (Ade-Cre). BMK1-deficient (Cre-treated $BMK1^{flox/flox}$) fibroblasts proliferated at about the same rate as BMK1-containing (Cre-treated $BMK1^{flox/+}$) fibroblasts (Figure 7B, left panel). The growth of BMK1-containing ECs appeared to be normal, and, in contrast, BMK1-deficient ECs not only stopped growing, but the number of viable cells also dropped significantly with time, an indication of cell death. Introduction of exogenous BMK1 by superinfecting recombinant adenovirus encoding BMK1 (Ade-BMK1) rescued Cre-treated $BMK1^{flox/flox}$ ECs from death (Figure 7B, right panel). Analysis of these ECs by TUNEL assay revealed that ablation of BMK1 induces profound EC apoptosis, and expression of exogenous BMK1 can rescue BMK1-

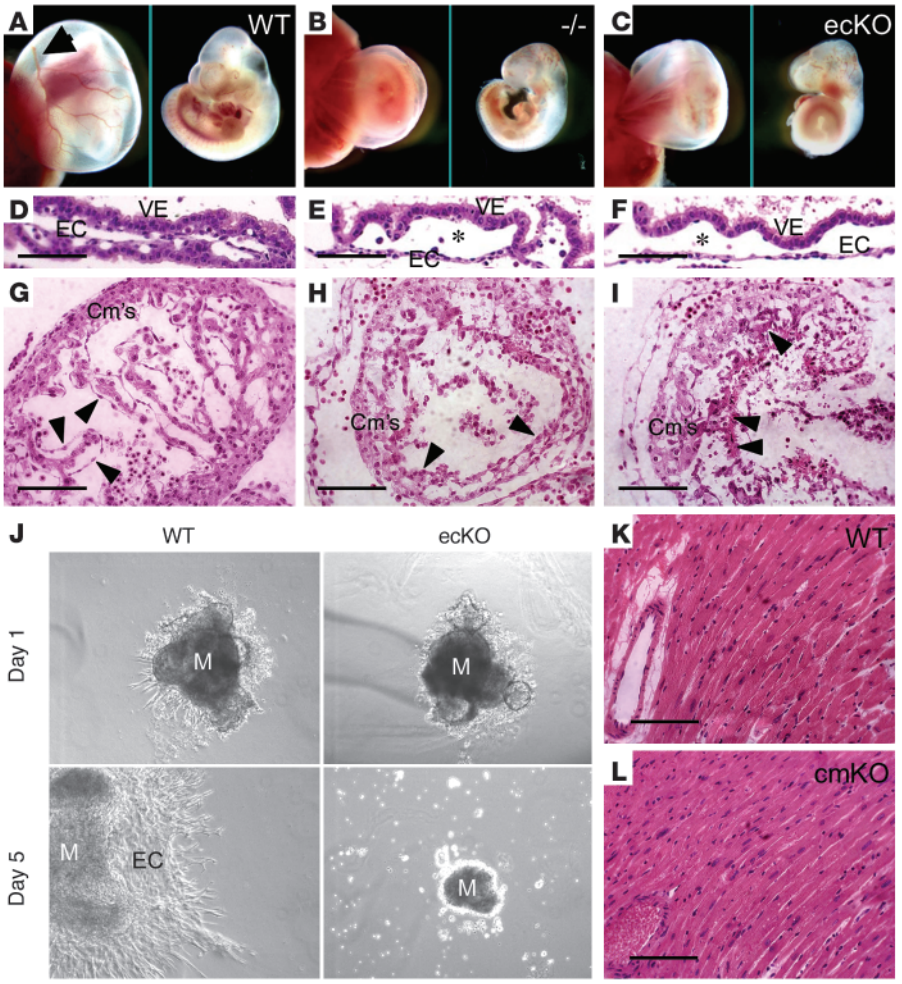

Figure 6
Essential role of BMK1 in ECs but not in cardiomyocytes during embryogenesis. (**A**–**C**) Growth retardation of global BMK1-KO (*BMK1*$^{-/-}$) and endothelial-specific BMK1-KO (BMK1-ecKO) embryos. Gross appearance of yolk sacs (left panel) and embryos (right panel) from WT (**A**), *BMK1*$^{-/-}$ (–/–) (**B**), and BMK1-ecKO (ecKO) (**C**) mutants at E9.5 are shown. Arrow in **A** indicates the major vitelline vessels, which are barely detectable in *BMK1*$^{-/-}$ and BMK1-ecKO mutants. (**D**–**F**) H&E staining of yolk sac of WT (**D**), *BMK1*$^{-/-}$ (**E**), and BMK1-ecKO (**F**) mutants at E9.5. Note that the vessels of the *BMK1*$^{-/-}$ and BMK1-ecKO yolk sacs are dilated compared with the vessels of the WT yolk sac. Asterisk denotes the underdeveloped vessels. (**G**–**I**) H&E staining of that hearts of WT (**G**), *BMK1*$^{-/-}$ (**H**), and BMK1-ecKO (**I**) mutants at E9.5. Arrowheads indicate ECs. (**J**) Deficit in endothelial proliferation in BMK1-ecKO heart explant cultures. (**K** and **L**) H&E staining of sections from WT and BMK1-cmKO (cmKO) hearts. M, myocardium; VE, visceral endoderm. Scale bars: **D**–**I**, **K**, and **L**, 10 μm.

mediated EC apoptosis (Figure 7C). Since VEGF, a strong EC survival factor, functions as a potent activator for BMK1 in ECs, BMK1 is likely responsible for transmitting VEGF-dependent antiapoptotic signals. Loss of BMK1, however, may cause the downregulation of VEGF receptors through transcriptional regulation, resulting in EC apoptosis by inhibiting VEGF-mediated survival signaling (31–33). To address this issue, the expression level of EC-specific growth factor receptors, including VEGF receptors, were analyzed. No difference was found between Cre-treated *BMK1*$^{flox/+}$ and *BMK1*$^{flox/flox}$ ECs (Figure 7D).

BMK1 delivers EC survival signal through its substrate MEF2C. Transcriptional factor MEF2C is a downstream target of BMK1, and the MEF2C-KO mutants also died around E9.5 with cardiovascular defects resembling those in the BMK1-ecKO mutant (14–16). This evidence raises the possibility that the BMK1/MEF2C pathway might play an indispensable role in supporting the function and/or survival of ECs. We first examined whether activation of BMK1 leads to upregulation of MEF2C transactivating activity in ECs using GAL4 *trans*-reporter assays. A substantial BMK1-dependent activation of MEF2C was observed in both HUVECs and MLCECs when the BMK1 pathway was specifically activated by MEK-5(D), a dominant active form of MEK-5 (Figure 8A). Serum provides EC survival signals and is also a potent activator for MEF2C in various cell types such as C2C12, CHO-K1, and COS-7 (1). To determine the relative contribution of the BMK1 pathway for serum-induced MEF2C activation in ECs, *BMK1*$^{flox/flox}$ MLCECs were used in MEF2C-dependent *trans*-reporter assays. Upon exposure to serum, BMK1-containing ECs exhibited a 3.5-fold induction of MEF2C-dependent reporter activity (Figure 8B). In contrast, this serum-mediated MEF2C activation was completely abolished in BMK1-deficient ECs. Moreover, superinfecting these ECs with Ade-BMK1 to provide them with exogenous BMK1 efficiently restored the serum-dependent MEF2C activation of these cells. The promoter region of *c-Jun* gene contains a MEF2 site that is required for serum-induced c-Jun expression. To further elucidate whether BMK1 regulates endogenous MEF2C activity, we used a MEF2-dependent *cis*-reporter assay in which the luciferase reporter gene is driven by either the WT c-Jun promoter (pJLuc) or a mutated MEF2 site containing the c-Jun promoter (pJSXLuc). Serum induced luciferase expression driven by the WT c-Jun promoter but failed to stimulate luciferase expression driven by the mutant c-Jun promoter (Figure 8C) in BMK1 containing ECs, indicating MEF2 activity is critical for serum-dependent c-Jun induction in ECs. Importantly, ablation of BMK1 abolished luciferase expression of pJLuc reporter gene induced by serum in MLCECs (Figure 8C) suggesting BMK1 is crucial for activating MEF2-dependent de novo transcription from serum induction. The

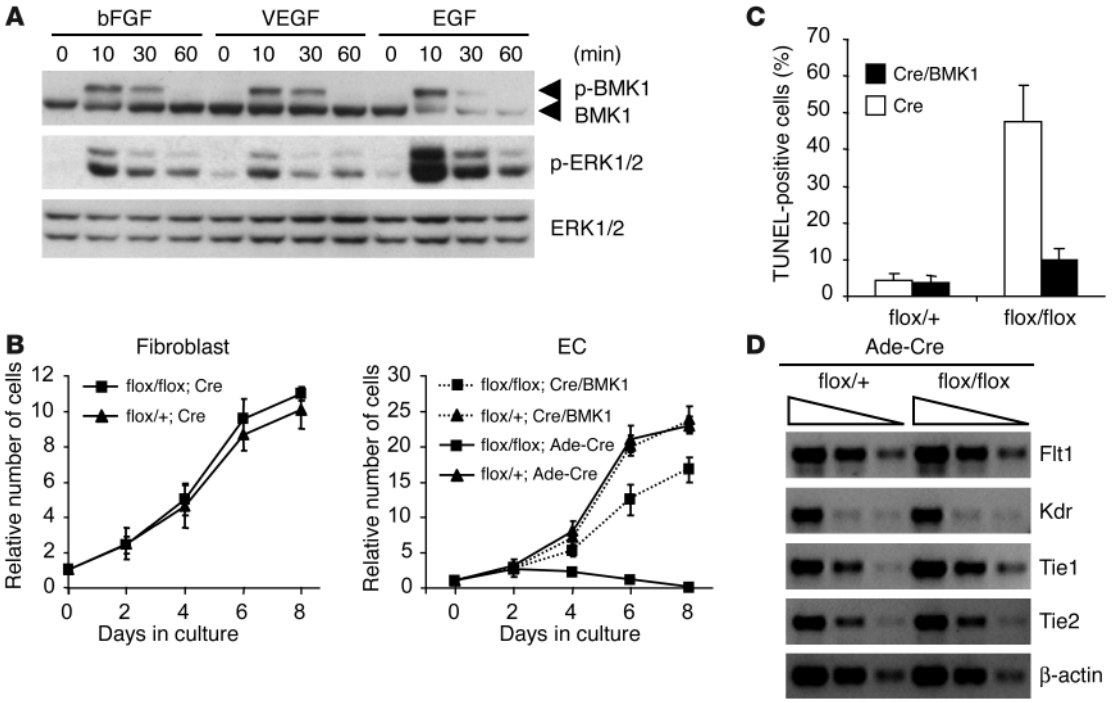

Figure 7
Requirement of BMK1 for the survival of ECs. (**A**) Activation of BMK1 in ECs by angiogenic growth factors. After 24-hour serum starvation, ECs were stimulated with 10 ng/ml of growth factors for the interval indicated. p-BMK1, phospho-BMK1; p–ERK1/2, phospho–ERK1/2. (**B**) Growth curves of *BMK1*$^{flox/+}$ and *BMK1*$^{flox/flox}$ fibroblast and EC cultures infected with either Ade-Cre or Ade-Cre along with Ade-BMK1 (Cre/BMK1). (**C**) Apoptosis in *BMK1*$^{flox/+}$ and *BMK1*$^{flox/flox}$ EC cultures infected with Cre or Cre/BMK1 adenovirus scored by TUNEL assay. (**D**) Semiquantitative RT-PCR for VEGF and angiopoietin receptor. RNA samples are from *BMK1*$^{flox/+}$ and *BMK1*$^{flox/flox}$ ECs infected with Cre-expressing adenovirus. A progression of fourfold dilutions of first-strand cDNA was used in each PCR to amplify gene products of Flt1, Kdr, Tie1, Tie2, and β-actin.

antiapoptotic role of MEF2C has been demonstrated in both primary cells and established cell lines (8, 34, 35). We suspected that BMK1-mediated MEF2C activation provides ECs with survival signal and that introduction of activated MEF2C could rescue EC apoptosis resulting from BMK1 removal. MLCECs were first treated with Ade-Cre followed by transfection of expression plasmid encoding constitutively active MEF2C (MEF2C-VP16) in which the DNA-binding and dimerization domain of MEF2C was fused to VP16 (36). Expression of MEF2C-VP16 in BMK1-deficient ECs provided considerable protection from apoptosis for these cells (Figure 8C). Taken together, these results suggest that BMK1 pathway delivers survival signal through MEF2C in ECs.

Discussion

Vascular permeability is an important indicator for the physiological status of blood vessels. Increases in microvascular permeability have been demonstrated in a number of systemic diseases (e.g., diabetes, hypertension, and rheumatoid arthritis) (37). Inflammatory mediators (e.g., histamine, serotonin, and bradykinin), VEGF, and shear stress have been shown to increase vascular permeability (38, 39). The mechanisms leading to the increased permeability are thought to occur either by passing through openings between adjacent ECs (intercellular) or by passing through the peripheral cytoplasm of ECs (transcellular) (37). We observed increased vascular leakage of Evans blue dye in BMK1-CKO mice as early as 1 week after induction of Cre recombinase when no hemorrhages were found in any organs. The increased leakage after BMK1 ablation is probably partially due to the increased permeability of ECs through transcellular openings, since numerous vesicles and vacuoles were found in a number of ECs (Figure 5C). It is still possible, however, that some of the leakage might pass through intercellular openings because complicated arrangements of fingerlike processes that interleave with each other were also found in the ultrastructural analysis of the capillaries.

The survival of ECs is vital for the maintenance of vasculature integrity. Growth factors such as VEGF, bFGF, and angiopoietin-1 are recognized to sustain EC survival by preventing EC apoptosis (40–42). The inhibition of EC apoptosis by these growth factors is shown to be dependent on the activation of intracellular PI3K/Akt signaling pathway (31, 43, 44) and may also be dependent on the upregulation of antiapoptotic proteins such as survivin and Bcl-2 (43–45). Herein, we demonstrated that in addition to PI3K/Akt, the BMK1 pathway is also required for EC survival, possibly through transmitting essential antiapoptotic signals from extracellular agonists. Besides the survival signals from endothelial growth factors, however, EC matrix and/or EC-EC contacts also have been shown to support cell survival (46, 47). Therefore, the role of the BMK1 pathway in integrands or EC homophilic adhesion-mediated antiapoptotic signaling needs to be elucidated.

Other than growth factors, oxidative stress is also a major activator for the BMK1 pathway (48, 49). Reactive oxygen species are known to play a critical role in inducing apoptosis, and highly reactive oxygen species levels have been detected in a number of

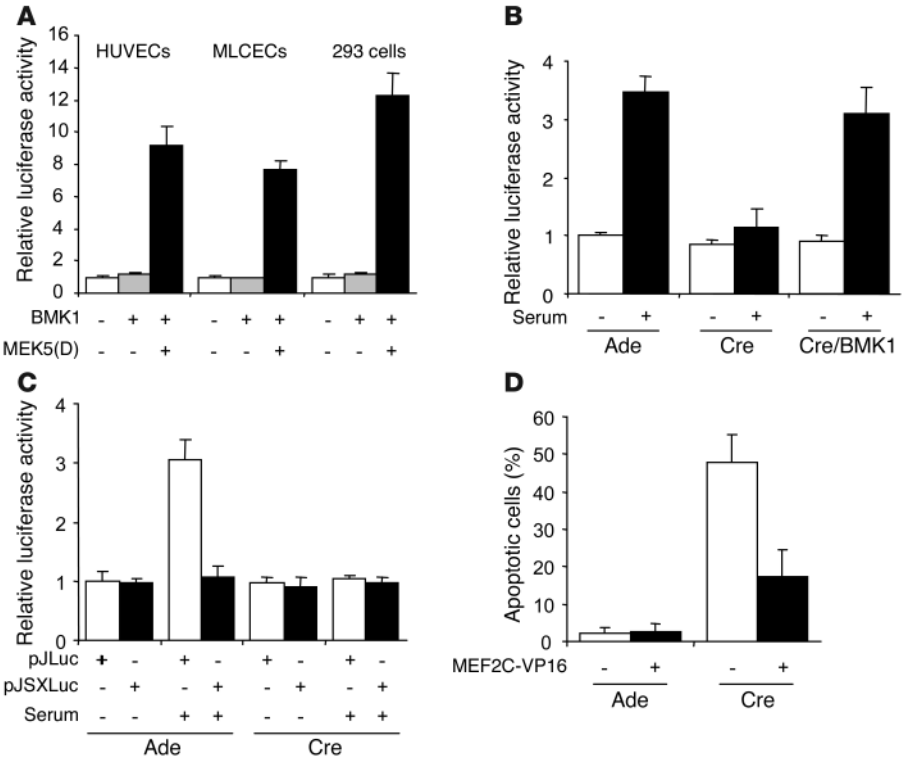

Figure 8

BMK1-mediated MEF2C activation is required for EC survival. (**A**) BMK1 stimulates MEF2C transactivation activity in ECs. HUVECs, MLCECs, and 293 cells were cotransfected with reporter plasmid pG5ElbLuc and GAL4-MEF2C. Additionally, control vector pcDNA3 or expression plasmids encoding MEK5(D) along with BMK1 were included in each transfection as indicated. (**B** and **C**) BMK1 mediates serum-induced MEF2C activation. MLCECs were first infected with adenovirus as indicated and were cotransfected with pG5E1bLuc and GAL4-MEF2C (**B**) or transfected with either pJLuc or pJSXLuc, *cis*-reporter plasmids of MEF2 element (**C**). Cells were then starved for 24 hours and stimulated with 10% serum for 6 hours before harvesting. (**D**) Expression of constitutively active MEF2C (MEF2C-VP16) rescued EC apoptosis caused by BMK1 deficiency. MLCECs were first infected with adenovirus as indicated and were cotransfected with GFP vector along with either control vector or MEF2C-VP16. Apoptosis in the transfected cell population (GFP-positive cells) was determined by cellular morphology 2 days after transfection. The data represent mean ± SEM of at least three independent transfections.

human diseases such as aging, ischemia, cancer, atherosclerosis, and neurodegenerative disease (50–54). The activation of BMK1 has been demonstrated to provide the survival signal for neutralizing cellular damage caused by oxidative insults (35). It is of interest to investigate whether the BMK1 pathway also provides survival signal for ECs to prevent the pathogenesis of human disorders caused by oxidative injury.

The mechanism linking the apoptosis of ECs to the formation of lumplike masses in heart tissues is unknown (Figure 4A). These masses, however, are clearly not generated by the defects of cardiomyocytes lacking BMK1, since the efficiency of Cre-mediated recombination in these cells is extremely low. Moreover, data from BMK1-cmKO mice strongly support the notion that BMK1 is not required for cardiac development and baseline function. One of the explanations is that the heart may be a unique tissue in which minor, repetitive mechanical injury to the already weakened ECs of BMK1-CKO mice produces repeated hemorrhaging, which, in combination with the consequential inflammation, leads to the generation of these masses. In addition, other genetic and physiological factors such as the embryologic origin of cardiac ECs, blood flow variation in different vessel types, as well as cardiac tissue oxygenation level, may also contribute to these differential phenotypes.

Any given MAPK contributes to the specificity of cellular responses, in part, through its particular downstream substrates. To date, many downstream targets of BMK1 have been identified, and, among them, the members of the MEF2 family of transcriptional factors are the best-characterized targets (1, 55). This family of transcriptional factors is composed of four members that were initially found as muscle-specific DNA-binding proteins, which recognized MEF2 motifs located inside the promoters of a number of muscle-specific genes (56). Phosphorylation of MEF2 by BMK1 activates MEF2. This activation has been shown to be critical for growth factor–induced neuronal survival (8, 9). In mice, MEF2C is expressed in developing cardiomyocytes, ECs, and smooth muscle cells, as well as in the surrounding mesenchyme, during embryogenesis. Disruption of the *MEF2C* locus leads to cardiovascular defects (14–16) bearing striking similarity to the embryonic abnormality observed in the BMK1-deficient mutant. The fact that activated MEF2C can partially rescue EC apoptosis caused by BMK1 removal further supports the concept that the BMK1 pathway relays its antiapoptotic signal within ECs through activating its downstream target MEF2C. The partial rescue of EC apoptosis suggests, however, that other mechanisms might also be involved, such as BMK1-dependent phosphorylation of Bcl2 antagonist of cell death (Bad), which was most recently described by Berk's lab (57).

The malfunction of both ECs and myocardiac cells has been suspected to play a part for the cardiovascular defects observed in BMK1-KO mutants (11, 12). These complex phenotypes of the conventional BMK1-KO mutant lead to fatalities in embryos, making it difficult to distinguish them from primary to secondary phenomena. We have circumvented this dilemma by generating mice with BMK1 ablation specifically in endothelium or in cardiac myocytes. EC-specific BMK1-KO mutant reproduced the cardiovascular defect of BMK1-KO mice, while cardiomyocyte-specific BMK1 KO mice developed normally and survived for more than 1 year without any cardiac complication. These results strongly suggest that BMK1 is essential for the function of ECs and the cardiac defects observed in conventional BMK1-KO mice is a secondary event resulting from dysfunctional ECs. Although BMK1-cmKO mice appear to be normal, suggesting that the BMK1 pathway is not critical for development and gen-

eral maintenance of cardiomyocytes, a number of studies have shown that the BMK1 pathway plays a role in various pathogenic processes of cardiac disease involving cardiomyocyte (58–60). Currently, we are evaluating the function of BMK1 in cardiomyocytes under stressed conditions using BMK1-cmKO mice.

In conclusion, we have shown that conditional ablation of BMK1 in adult mice results in defects of vascular integrity and endothelial maintenance. Moreover, we have also demonstrated in vitro that an intact signaling pathway in BMK1 is essential for EC survival. The phenotype observed here is of particular interest since, thus far, no genetic model with "endothelial failure" in the adult stage has been demonstrated. Moreover, the role for endothelial apoptosis as a mechanism for the effect of BMK1 inhibition in ECs may facilitate the design of effective therapy to enhance angiogenesis in diseases of tissue ischemia or inhibit angiogenesis in diseases dependent on neovascularization.

Acknowledgments

We thank Kent Osborn (The Scripps Research Institute) and Malcolm Wood (The Scripps Research Institute) for their expertise on pathology and electron microscope, respectively. This work was supported by funds from National Cancer Institute (to J.-D. Lee), Department of Defense Prostate Cancer Research Program (to J.-D. Lee), and by a fellowship from California Breast Cancer Research Program (to M. Hayashi).

Received for publication August 27, 2003, and accepted in revised form January 28, 2004.

Address correspondence to: Jiing-Dwan Lee, Department of Immunology, The Scripps Research Institute, La Jolla, California 92037, USA. Phone: (858) 784-8703; Fax: (858) 784-8343; E-mail: jdlee@scripps.edu.

1. Kato, Y., et al. 1997. BMK1/ERK5 regulates serum-induced early gene expression through transcription factor MEF2C. *EMBO J.* **16**:7054–7066.
2. Chao, T.H., Hayashi, M., Tapping, R.I., Kato, Y., and Lee, J.D. 1999. MEKK3 directly regulates MEK5 activity as part of the big mitogen-activated protein kinase 1 (BMK1) signaling pathway. *J. Biol. Chem.* **274**:36035–36038.
3. English, J.M., Vanderbilt, C.A., Xu, S., Marcus, S., and Cobb, M.H. 1995. Isolation of MEK5 and differential expression of alternatively spliced forms. *J. Biol. Chem.* **270**:28897–28902.
4. Zhou, G., Bao, Z.Q., and Dixon, J.E. 1995. Components of a new human protein kinase signal transduction pathway. *J. Biol. Chem.* **270**:12665–12669.
5. Kato, Y., et al. 1998. Bmk1/Erk5 is required for cell proliferation induced by epidermal growth factor. *Nature.* **395**:713–716.
6. English, J.M., et al. 1999. Contribution of the ERK5/MEK5 pathway to Ras/Raf signaling and growth control. *J. Biol. Chem.* **274**:31588–31592.
7. Kamakura, S., Moriguchi, T., and Nishida, E. 1999. Activation of the protein kinase ERK5/BMK1 by receptor tyrosine kinases. Identification and characterization of a signaling pathway to the nucleus. *J. Biol. Chem.* **274**:26563–26571.
8. Liu, L., et al. 2003. ERK5 activation of MEF2-mediated gene expression plays a critical role in BDNF-promoted survival of developing but not mature cortical neurons. *Proc. Natl. Acad. Sci. U. S. A.* **100**:8532–8537.
9. Watson, F.L., et al. 2001. Neurotrophins use the ERK5 pathway to mediate a retrograde survival response. *Nat. Neurosci.* **4**:981–988.
10. Dinev, D., et al. 2001. Extracellular signal regulated kinase 5 (ERK5) is required for the differentiation of muscle cells. *EMBO Rep.* **2**:829–834.
11. Regan, C.P., et al. 2002. Erk5 null mice display multiple extraembryonic vascular and embryonic cardiovascular defects. *Proc. Natl. Acad. Sci. U. S. A.* **99**:9248–9253.
12. Sohn, S.J., Sarvis, B.K., Cado, D., and Winoto, A. 2002. ERK5 MAPK regulates embryonic angiogenesis and acts as a hypoxia-sensitive repressor of vascular endothelial growth factor expression. *J. Biol. Chem.* **277**:43344–43351.
13. Yang, J., et al. 2000. Mekk3 is essential for early embryonic cardiovascular development. *Nat. Genet.* **24**:309–313.
14. Lin, Q., Schwarz, J., Bucana, C., and Olson, E.N. 1997. Control of mouse cardiac morphogenesis and myogenesis by transcription factor MEF2C. *Science.* **276**:1404–1407.
15. Lin, Q., et al. 1998. Requirement of the MADS-box transcription factor MEF2C for vascular development. *Development.* **125**:4565–4574.
16. Bi, W., Drake, C.J., and Schwarz, J.J. 1999. The transcription factor MEF2C-null mouse exhibits complex vascular malformations and reduced cardiac expression of angiopoietin 1 and VEGF. *Dev. Biol.* **211**:255–267.
17. Adams, R.H., et al. 2000. Essential role of p38alpha MAP kinase in placental but not embryonic cardiovascular development. *Mol. Cell.* **6**:109–116.
18. Tamura, K., et al. 2000. Requirement for p38alpha in erythropoietin expression: a role for stress kinases in erythropoiesis. *Cell.* **102**:221–231.
19. Kuhn, R., Schwenk, F., Aguet, M., and Rajewsky, K. 1995. Inducible gene targeting in mice. *Science.* **269**:1427–1429.
20. Rodriguez, C.I., et al. 2000. High-efficiency deleter mice show that FLPe is an alternative to Cre-loxP. *Nat. Genet.* **25**:139–140.
21. Meyers, E.N., Lewandoski, M., and Martin, G.R. 1998. An Fgf8 mutant allelic series generated by Cre- and Flp-mediated recombination. *Nat. Genet.* **18**:136–141.
22. Jat, P.S., et al. 1991. Direct derivation of conditionally immortal cell lines from an H-2Kb-tsA58 transgenic mouse. *Proc. Natl. Acad. Sci. U. S. A.* **88**:5096–5100.
23. Koni, P.A., et al. 2001. Conditional vascular cell adhesion molecule 1 deletion in mice: impaired lymphocyte migration to bone marrow. *J. Exp. Med.* **193**:741–754.
24. Abel, E.D., et al. 1999. Cardiac hypertrophy with preserved contractile function after selective deletion of GLUT4 from the heart. *J. Clin. Invest.* **104**:1703–1714.
25. Lobe, C.G., et al. 1999. Z/AP, a double reporter for cre-mediated recombination. *Dev. Biol.* **208**:281–292.
26. Camenisch, T.D., et al. 2000. Disruption of hyaluronan synthase-2 abrogates normal cardiac morphogenesis and hyaluronan-mediated transformation of epithelium to mesenchyme. *J. Clin. Invest.* **106**:349–360.
27. Serrano, M., Lin, A.W., McCurrach, M.E., Beach, D., and Lowe, S.W. 1997. Oncogenic ras provokes premature cell senescence associated with accumulation of p53 and p16INK4a. *Cell.* **88**:593–602.
28. Brutsaert, D.L. 2003. Cardiac endothelial-myocardial signaling: its role in cardiac growth, contractile performance, and rhythmicity. *Physiol. Rev.* **83**:59–115.
29. Ferrara, N., et al. 1996. Heterozygous embryonic lethality induced by targeted inactivation of the VEGF gene. *Nature.* **380**:439–442.
30. Cines, D.B., et al. 1998. Endothelial cells in physiology and in the pathophysiology of vascular disorders. *Blood.* **91**:3527–3561.
31. Gerber, H.P., et al. 1998. Vascular endothelial growth factor regulates endothelial cell survival through the phosphatidylinositol 3′-kinase/Akt signal transduction pathway. Requirement for Flk-1/KDR activation. *J. Biol. Chem.* **273**:30336–30343.
32. Tran, J., et al. 2002. A role for survivin in chemoresistance of endothelial cells mediated by VEGF. *Proc. Natl. Acad. Sci. U. S. A.* **99**:4349–4354.
33. Carmeliet, P., et al. 1999. Targeted deficiency or cytosolic truncation of the VE-cadherin gene in mice impairs VEGF-mediated endothelial survival and angiogenesis. *Cell.* **98**:147–157.
34. Okamoto, S., Krainc, D., Sherman, K., and Lipton, S.A. 2000. Antiapoptotic role of the p38 mitogen-activated protein kinase-myocyte enhancer factor 2 transcription factor pathway during neuronal differentiation. *Proc. Natl. Acad. Sci. U. S. A.* **97**:7561–7566.
35. Suzaki, Y., et al. 2002. Hydrogen peroxide stimulates c-Src-mediated big mitogen-activated protein kinase 1 (BMK1) and the MEF2C signaling pathway in PC12 cells: potential role in cell survival following oxidative insults. *J. Biol. Chem.* **277**:9614–9621.
36. Molkentin, J.D., Black, B.L., Martin, J.F., and Olson, E.N. 1996. Mutational analysis of the DNA binding, dimerization, and transcriptional activation domains of MEF2C. *Mol. Cell Biol.* **16**:2627–2636.
37. Michel, C.C., and Curry, F.E. 1999. Microvascular permeability. *Physiol. Rev.* **79**:703–761.
38. Dvorak, H.F., Brown, L.F., Detmar, M., and Dvorak, A.M. 1995. Vascular permeability factor/vascular endothelial growth factor, microvascular hyperpermeability, and angiogenesis. *Am. J. Pathol.* **146**:1029–1039.
39. Feng, D., Nagy, J.A., Hipp, J., Dvorak, H.F., and Dvorak, A.M. 1996. Vesiculo-vacuolar organelles and the regulation of venule permeability to macromolecules by vascular permeability factor, histamine, and serotonin. *J. Exp. Med.* **183**:1981–1986.
40. Alon, T., et al. 1995. Vascular endothelial growth factor acts as a survival factor for newly formed retinal vessels and has implications for retinopathy of prematurity. *Nat. Med.* **1**:1024–1028.
41. Kwak, H.J., So, J.N., Lee, S.J., Kim, I., and Koh, G.Y. 1999. Angiopoietin-1 is an apoptosis survival factor for endothelial cells. *FEBS Lett.* **448**:249–253.
42. Karsan, A., et al. 1997. Fibroblast growth factor-2 inhibits endothelial cell apoptosis by Bcl-2-dependent and independent mechanisms. *Am. J. Pathol.* **151**:1775–1784.
43. Fujio, Y., and Walsh, K. 1999. Akt mediates cytoprotection of endothelial cells by vascular endothelial growth factor in an anchorage-dependent manner. *J. Biol. Chem.* **274**:16349–16354.
44. Papapetropoulos, A., et al. 2000. Angiopoietin-1 inhibits endothelial cell apoptosis via the Akt/survivin pathway. *J. Biol. Chem.* **275**:9102–9105.

45. O'Connor, D.S., et al. 2000. Control of apoptosis during angiogenesis by survivin expression in endothelial cells. *Am. J. Pathol.* **156**:393–398.
46. Meredith, J.E., Jr., Fazeli, B., and Schwartz, M.A. 1993. The extracellular matrix as a cell survival factor. *Mol. Biol. Cell.* **4**:953–961.
47. Bird, I.N., et al. 1999. Homophilic PECAM-1(CD31) interactions prevent endothelial cell apoptosis but do not support cell spreading or migration. *J. Cell Sci.* **112**(Pt 12):1989–1997.
48. Abe, J., Kusuhara, M., Ulevitch, R.J., Berk, B.C., and Lee, J.D. 1996. Big mitogen-activated protein kinase 1 (BMK1) is a redox-sensitive kinase. *J. Biol. Chem.* **271**:16586–16590.
49. Abe, J., Takahashi, M., Ishida, M., Lee, J.D., and Berk, B.C. 1997. c-Src is required for oxidative stress-mediated activation of big mitogen-activated protein kinase 1. *J. Biol. Chem.* **272**:20389–20394.
50. Johnson, F.B., Sinclair, D.A., and Guarente, L. 1999. Molecular biology of aging. *Cell.* **96**:291–302.
51. Irani, K. 2000. Oxidant signaling in vascular cell growth, death, and survival: a review of the roles of reactive oxygen species in smooth muscle and endothelial cell mitogenic and apoptotic signaling. *Circ. Res.* **87**:179–183.
52. Cleveland, J.L., and Kastan, M.B. 2000. Cancer. A radical approach to treatment. *Nature.* **407**:309–311.
53. Prasad, K.N., et al. 2000. Multiple antioxidants in the prevention and treatment of Alzheimer disease: analysis of biologic rationale. *Clin. Neuropharmacol.* **23**:2–13.
54. Giasson, B.I., et al. 2000. Oxidative damage linked to neurodegeneration by selective alpha-synuclein nitration in synucleinopathy lesions. *Science.* **290**:985–989.
55. Kato, Y., et al. 2000. Big mitogen-activated kinase regulates multiple members of the MEF2 protein family. *J. Biol. Chem.* **275**:18534–18540.
56. Black, B.L., and Olson, E.N. 1998. Transcriptional control of muscle development by myocyte enhancer factor-2 (MEF2) proteins. *Annu. Rev. Cell Dev. Biol.* **14**:167–196.
57. Pi, X., Yan, C., and Berk, B.C. 2004. Big mitogen-activated protein kinase (BMK1)/ERK5 protects endothelial cells from apoptosis. *Circ. Res.* **94**:362–369.
58. Nicol, R.L., et al. 2001. Activated MEK5 induces serial assembly of sarcomeres and eccentric cardiac hypertrophy. *EMBO J.* **20**:2757–2767.
59. Nakaoka, Y., et al. 2003. Activation of gp130 transduces hypertrophic signal through interaction of scaffolding/docking protein Gab1 with tyrosine phosphatase SHP2 in cardiomyocytes. *Circ. Res.* **93**:221–229.
60. Kacimi, R., and Gerdes, A.M. 2003. Alterations in G protein and MAP kinase signaling pathways during cardiac remodeling in hypertension and heart failure. *Hypertension.* **41**:968–977.